



## Application of a rotating packed bed contactor for removal of Direct Red 23 by adsorption

Anirban Kundu<sup>a</sup>, Lili Shakira Hassan<sup>b</sup>, Ghufran Redzwan<sup>a</sup>, Desmond Robinson<sup>b</sup>, Mohd. Ali Hashim<sup>c</sup>, Bhaskar SenGupta<sup>d,\*</sup>

<sup>a</sup>Institute of Biological Sciences, University of Malaya, Kuala Lumpur 50603, Malaysia, Tel. +60379676797; emails: [kundu.anirban@yahoo.com](mailto:kundu.anirban@yahoo.com) (A. Kundu), [ghufran@um.edu.my](mailto:ghufran@um.edu.my) (G. Redzwan)

<sup>b</sup>School of Planning, Architecture and Civil Engineering, Queen's University Belfast, David Keir Building, Belfast, BT9 5AG, UK, Tel. +44 0 28 9097 4025; emails: [leelyhassan@gmail.com](mailto:leelyhassan@gmail.com) (L. Shakira Hassan), [des.robinson@qub.ac.uk](mailto:des.robinson@qub.ac.uk) (D. Robinson)

<sup>c</sup>Department of Chemical Engineering, University of Malaya, Kuala Lumpur 50603, Malaysia, Tel. +60379675296; email: [alhashim@um.edu.my](mailto:alhashim@um.edu.my)

<sup>d</sup>Water Academy, School of the Built Environment, Heriot-Watt University, Edinburgh Campus, EH14 4AS Scotland, Tel. +44 0 131 451 8171; email: [b.sengupta@hw.ac.uk](mailto:b.sengupta@hw.ac.uk)

Received 7 November 2014; Accepted 3 June 2015

### ABSTRACT

In this work, a rotating packed bed (RPB) contactor was applied to adsorb Direct Red 23 dye onto commercially available activated carbon. A RPB is a doughnut shaped contactor, which rotates on a vertical axis and centrifugal force acts as the driving force for fluid-particle contact in the contactor. This centrifugal force, which is several times higher than the gravitational force, aids the adsorption process with enhanced mass transfer coefficient. The commercially available activated carbon used in this work had moderate BET surface area of  $583 \text{ m}^2 \text{ g}^{-1}$  and was mainly meso-porous with an average pore size of  $22 \text{ \AA}$ . The adsorption characteristics of the activated carbon were studied in a shake flask and a RPB. The dye removal in RPB was 93% compared to 55% in a shake flask in 5 h for the same amount of activated carbon and dye solution. Rotor speed and feed rate were important parameters for the removal of the dye in a RPB. It was found that rotor speed of 628 rpm and feed rate of  $40 \text{ L h}^{-1}$  yielded the best adsorption efficiency.

*Keywords:* Rotating packed bed; Process intensification; Adsorption; Activated carbon; Direct Red 23

### 1. Introduction

Industries such as textile, cosmetics and paper and pulp are known for producing large volumes of coloured effluent, which are difficult to treat due to the high chemical stability of dyes. Conventional physicochemical and biological treatment processes

often prove inadequate to meet the discharge standards of different countries. Some of the treatment processes like membrane filtration, electrochemical, photo oxidation and chemicals such as Fenton reagent or hypochlorite have been used to treat wastewater containing dye. However, all the processes have their own demerits associated with cost and sludge disposal [1–7].

\*Corresponding author.

Direct Red 23 (DR 23) is an azo dye that is commonly used to dye cotton fabrics [8]. According to Shore [9], it is highly toxic and carcinogenic in nature. Also, DR23 is not easily biodegraded. There are several studies on degradation of DR23 dye. Song et al. [10] studied the photo-catalytic degradation of DR23 in aqueous medium under UV irradiation using SrTiO<sub>3</sub>/CeO<sub>2</sub> composite as the catalyst. Song et al. [11] also studied the mechanism of decolourisation and degradation of DR23 by ozonation combined with sonolysis. Daneshvar et al. [12] experimented with immobilised TiO<sub>2</sub> nano-powder on glass beads for the photo-catalytic decolourisation of DR23. Sobana et al. [13] studied the optimised photo-catalytic degradation condition of DR23 using nano-Ag doped TiO<sub>2</sub>. Sohrabi and Ghavami [14] studied the effect of parameters for photo-catalytic degradation of DR23 dye using UV/TiO<sub>2</sub>. There are few studies on removal of DR23 specifically by adsorption. Lucilha et al. [15] studied adsorption of DR23 onto zinc oxide surface while Konicki et al. [16] conducted experimental investigation on adsorption onto magnetic multi-walled carbon nanotubes Fe<sub>3</sub>C nano-composite. Doulati Ardejani et al. [17] used orange peel, a low cost adsorbent, to remove the dye and also carried out numerical modelling of the process.

Current research is focussed on rapid adsorption of dye on commercially available activated carbon in a rotating packed bed (RPB). In this context, a RPB contactor can be used as an efficient adsorption system due to lowering of mass transfer resistance caused by high relative velocity between the solid and the flowing liquid. A RPB contactor was first designed by Ramshaw and Mallinson in the year 1981 to enhance mass transfer rate between two fluid phases [18,19]. RPB was termed as Hige as the gravitational field was replaced by the centrifugal force, which was several times higher in value than the gravitational force. A RPB contactor found applications in different process, where mass transfer is crucial, such as absorption, distillation, stripping, heat transfer, extraction and nanoparticles preparation [20–23]. Till now, the RPB has been utilised mostly for solid-gas or liquid-gas mass transfer processes [24–26]. It has hardly been used for adsorption of contaminants from wastewater. Adsorption of Basic Yellow 2 on activated carbon in centrifugal adsorption bed by Lin and Liu [27] showed that centrifugal acceleration had significant effect on the adsorption of the dyestuff. A pseudo-first-order model would provide a reasonable representation for the mechanism of adsorption of basic yellow dye on activated carbon. The intraparticle diffusion model could govern the rate-limiting step at the initial stages of adsorption. They concluded that

the centrifugal force would improve the overall mass transfer rate in the adsorption process, as it was evident that centrifugal force improved the rate constants, the intraparticle diffusion rate parameters, and the diffusion coefficients for the adsorption of basic yellow dye on the activated carbon. Das et al. [28] studied the mass transfer characteristics of continuous biosorption of Cu(II) ions on *Catla catla* fish scale under centrifugal acceleration in a RPB contactor. They reported enhancement in volumetric mass transfer coefficient with increasing rotor speed. Panda et al. [29] used crude tamarind (*Tamarindus indica*) fruit shell to remove hexavalent chromium ions from an aqueous solution in a RPB contactor by continuously recirculating a given volume of solution through the bed. In this study, it was reported that the transport rate of Cr(VI) ions increases with rotational speed due to reduced external phase mass transfer resistance. According to the study, the removal rate of Cr(VI) by TFS is influenced by diffusional resistances and can be improved by employing high liquid flow rate, rotational speed and reducing particle size.

The purpose of this study was to investigate the adsorption of DR23 dye on activated carbon in a RPB. This study investigated adsorption rates of the dye in a RPB and compared the results with the shake flask data for the same amount of activated carbon. Effect of operational parameters such as activated carbon loading, rotor speed and feed rate were studied to understand the influence of these parameters on dye adsorption.

## 2. Materials and methods

### 2.1. Adsorbent and adsorbate

Molecular formula for red dye 23 is C<sub>35</sub>H<sub>25</sub>N<sub>7</sub>Na<sub>2</sub>O<sub>10</sub>S<sub>2</sub> with molecular weight of 813.72 g mol<sup>-1</sup>. It has maximum absorption wavelength, λ<sub>max</sub> = 505 nm. Structure of DR23 is shown in Fig. 1. The dye was of reagent grade from Sigma-Aldrich and used without further purification. The activated carbon used in this study as adsorbent was obtained from Sigma-Aldrich and used without any modification. The particle size of the activated carbon was between 250 micrometer and 500 micrometer.

### 2.2. Characteristics of activated carbon

The activated carbon was characterised by scanning electron microscopy, Brunauer–Emmett–Teller (BET) surface area and FTIR spectroscopy as described by [30].

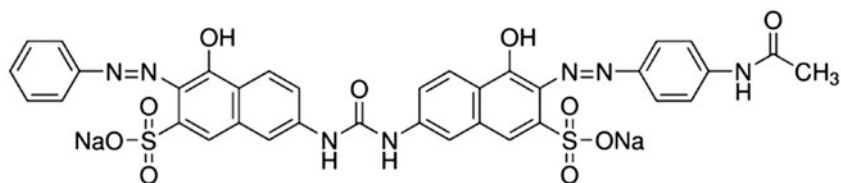


Fig. 1. Chemical structure of DR23.

### 2.3. RPB system

A RPB reactor was a doughnut shaped contactor that was rotated with the help of a motor as shown in Fig. 2. The rotor was annular shaped and the activated carbon was placed in the annular space at various packing densities. The height of the bed was 1 cm. The inner and outer radii of the rotor were 2 and 3.2 cm, respectively, having an annular space of 1.2 cm. The inner wall and outer walls were made up of stainless steel mesh of size 50 mm. Liquid was injected through a port on the inner wall of the rotor. As the rotor was rotated at high speed, the liquid was discharged from the outer wall. The liquid flow path is indicated in Fig. 2. In this study, the packed bed was rotated on a vertical axis. The rotor was driven by a 0.5 hp motor at a speed ranging from 100 to 2,000 rpm, thereby generating 0.3–112 times the gravitational force on the basis of the arithmetic mean radius.

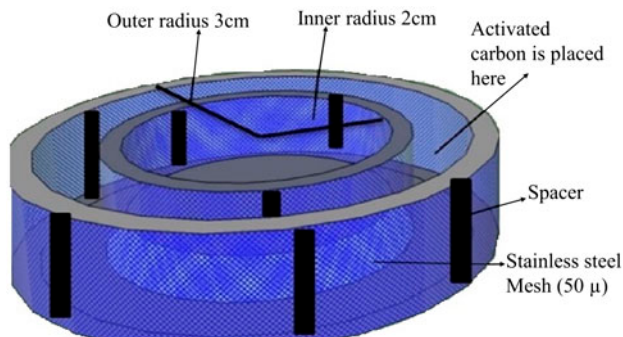


Fig. 3. Schematic diagramme of the rotating bed and how the carbon is fixed in the annular place.

### 2.4. Experimental procedures

DR23 dye was mixed thoroughly with distilled water to prepare solutions having concentrations of

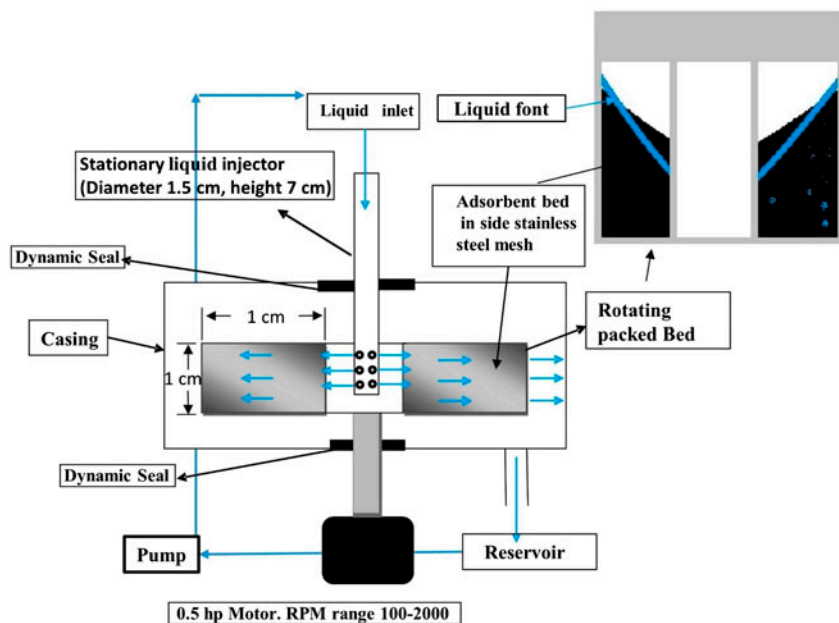


Fig. 2. Diagram of RPB (inset the liquid profile inside the RPB, liquid flow path is marked in blue).

50 and 100 mg L<sup>-1</sup>. The samples were marked as SF 50 and 100, respectively, and used for shake flask experiments. For each experiment, 200 mL of dye sample was taken in an Erlenmeyer flask and 2 g activated carbon was added to the flask and agitated in a shaker at 150 rpm. For analysis purpose, 4 mL sample was collected from the shake flask and centrifuged at 2,000 rpm to separate the solids from the liquid. Dye concentration was determined by the Perkin Elmer Lambda 35 UV/VIS spectrophotometer at the required wavelength. Dye solutions of 50 and 100 mg L<sup>-1</sup> concentration were prepared for this work shortly before the experiment, which were marked as RPB50 and RPB100, respectively. To study the effect of contact time, per cent removal of DR23 dye was observed for 24 h. The experimental conditions were: rotor speed 1,140 rpm, feed rate 40 L h<sup>-1</sup> and 10 g of activated carbon loading. The ratio of solid to liquid (10 g L<sup>-1</sup>) was maintained for both shake flask and RPB experiments. Samples were collected at 10 minutes interval for the first two hours and then at every one hour interval up to five hours and then collected at 8th, 12th, 16th, and 24th h from the start. The samples were collected from the reservoir by pipetting out 4 mL, required for spectrophotometric analysis. The sample containing both liquid and solid fractions was returned to the reservoir as soon as the measurement was over. In case of RPB, there was no need for any separation of liquid from the suspension, as all the solids remained inside the rotor. The amount of adsorbed DR23 at time  $t$ ,  $q_t$  (mg g<sup>-1</sup>) was calculated by the following equation:

$$q_t = \frac{(C_0 - C_t)V}{m} \quad (1)$$

where  $C_0$  (mg L<sup>-1</sup>) is the initial dye concentration,  $C_t$  (mg L<sup>-1</sup>) is the dye concentration at any time,  $t$ ,  $V$  (L) is the volume of solution and  $m$  (g) is the mass of the adsorbent.

The data obtained was then analysed with linearised form of pseudo-first-order kinetics and pseudo-second-order kinetics as represented by Eqs. (2) and (3) [30].

$$\ln(q_e - q_t) = \ln q_e - k_1 t \quad (2)$$

where  $k_1$  is the Lagergren rate constant of adsorption (min<sup>-1</sup>). The values of  $q_e$  and  $k_1$  were determined from the plot of  $\ln(q_e - q_t)$  against  $t$ .

$$\frac{t}{q_t} = \frac{1}{k_2 q_e^2} + \frac{t}{q_e} \quad (3)$$

where  $k_2$  is the pseudo-second-order rate constant of adsorption (g mg<sup>-1</sup> min<sup>-1</sup>). The values of the pseudo-second-order rate constants  $q_e$  and  $k_2$  were calculated from the slopes and intercepts of straight portion of the linear plots obtained by plotting  $t/q_t$  vs.  $t$ .

The  $q_{e, \text{exp}}$  was calculated from the experimental value at the 24 h and the  $q_{e, \text{cal}}$  was obtained from the plots as mentioned above for Eqs. (2) and (3).

In order to check the mechanism of the adsorption process, the intra-particle diffusion model suggested by Webber and Morris (1962) was examined. The initial rate of intra-particle diffusion was obtained by linear form of the Webber and Morris equation [31]:

$$q_t = k_t t^{0.5} \quad (4)$$

### 3. Result and discussion

#### 3.1. Characterisation of the activated carbon

The SEM image in Fig. 4 shows that the surface morphology of the activated carbon is quite rough and porous. Nitrogen adsorption/desorption isotherms determined the specific surface area from the BET equation. The BET surface area was found to be 583 m<sup>2</sup> g<sup>-1</sup>. The nitrogen adsorption/desorption plot shown in Fig. 5 suggests that the activated carbon can be characterised as mesoporous (monolayer adsorption only) with relatively small external surface area. The average pore diameter of the activated carbon was 22 Å.

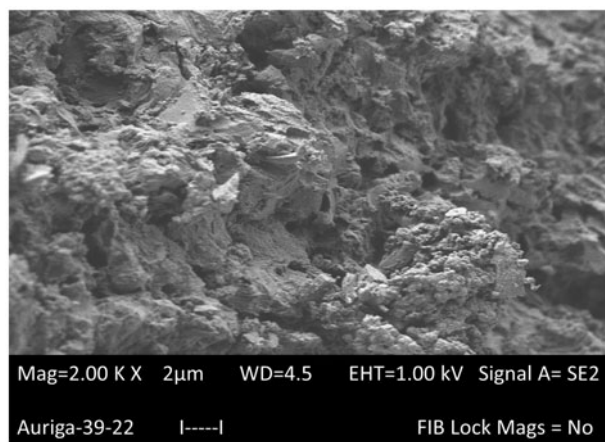


Fig. 4. SEM image of the activated carbon.

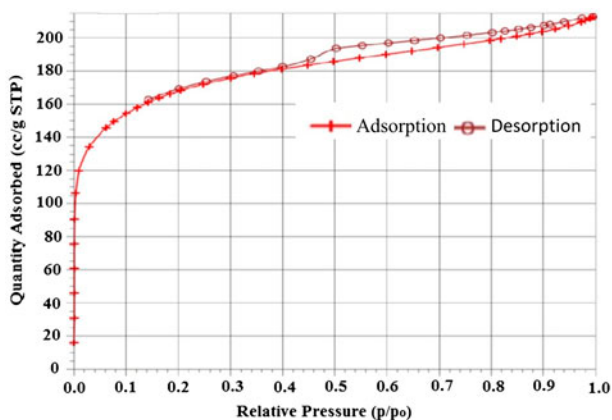


Fig. 5. Nitrogen adsorption/desorption plot for the activated carbon.

FTIR data shown in Fig. 6 indicate that the intensity of the peak between  $3,500$  and  $3,200\text{ cm}^{-1}$ , which is attributed to O–H stretching of alcohol group or phenol group present in the activated carbon. Intensity of the band of  $3,000$ – $2,850\text{ cm}^{-1}$  corresponding to C–H stretch of alkanes is very low, which suggests that these groups are not present in the activated carbon. The complex peaks around  $1,580$ – $1,650\text{ cm}^{-1}$  could be attributed to N–H bend of primary amines and C–C stretch of aromatic ring. The C–O stretch for alcohol group, carboxylic acid group and ester group corresponding to the bands  $1,300$ – $1,000\text{ cm}^{-1}$  are also present in the activated carbon.

### 3.2. Comparative study of dye removal with contact time in shake flask and in RPB

The effect of contact time on adsorption of dye keeping the same effluent to adsorbent ratio was stud-

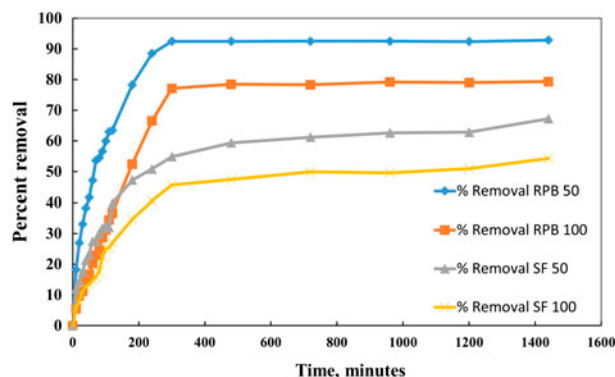


Fig. 7. Comparison dye removal in RPB and Shake flask.

ied for both RPB and shake flask to understand the effect of the centrifugal force on the adsorption of DR23. The data obtained is shown in Fig. 7. It can be observed clearly that removal percentage in RPB is much higher than that in the shake flask experiment. In five hours, per cent removal of dye reached 93% for  $50\text{ mg L}^{-1}$  initial concentration in RPB, while 77% of the dye was removed from  $100\text{ mg L}^{-1}$  solution in RPB. A removal of 55% for initial concentration  $50\text{ mg L}^{-1}$  and 46% for initial concentration of  $100\text{ mg L}^{-1}$  was observed for shake flask study, which were considerably lower than that for RPB in 5 h. The reason for higher removal in the RPB contactor is mainly attributed to lowering of mass transfer resistance caused by the centrifugal force generated due to high rotational speed of the bed [28,29]. This relative centrifugal force (RCF) can be several times higher than the gravitational force depending upon the rotating speed according to Eq. (5) [32]:

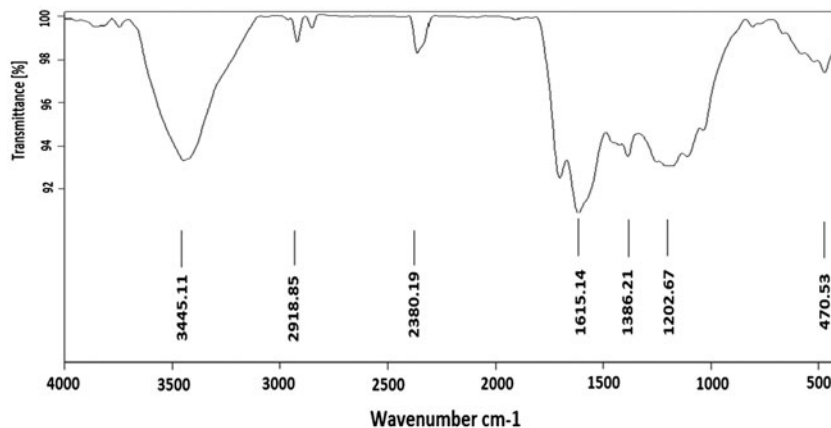


Fig. 6. FT-IR image of the activated carbon.

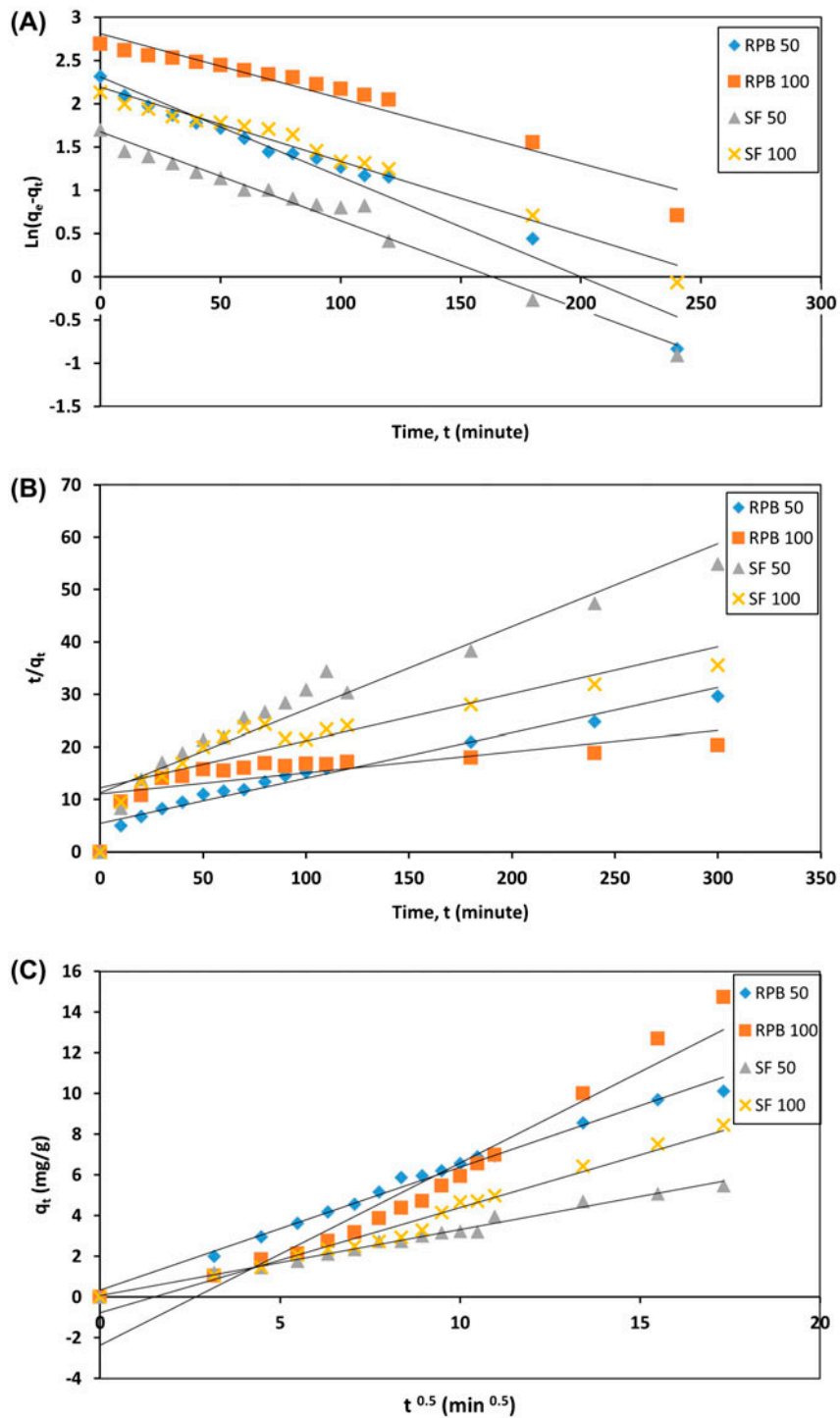


Fig. 8. (A) Pseudo-first-order kinetic model, (B) pseudo-second-order kinetic model and (C) intra-particle diffusion model for adsorption of DR23 on AC in RPB.

$$RCF = 11.18 \times r \times \left( \frac{Q}{1,000} \right)^2 \quad (5)$$

### 3.3. Kinetic studies for the adsorption of the dye

A linearised form of pseudo-first-order kinetic equation, popularly known as the Lagergren equation,

Table 1  
Pseudo-first-order, pseudo-second-order and intra-particle diffusion values

Experiments	Initial concentration (mg L <sup>-1</sup> )	$q_{e, \text{exp}}$ (mg/g)	Pseudo-first-order kinetic model			Pseudo-second-order kinetic model			Intra-particle diffusion	
			$q_{e, \text{cal}}$	$k_1$	$R^2$	$q_{e, \text{cal}}$	$k_2$	$R^2$	$k_{\text{ipd}}$	$R^2$
Rotating packed bed	50	10.12	10.1	0.012	0.9617	11.59	0.008	0.9431	0.604	0.9903
	100	14.73	16.63	0.008	0.9412	24.94	0.003	0.4866	0.896	0.9435
Shake flask	50	5.47	5.34	0.010	0.9738	6.32	0.027	0.9125	0.324	0.9878
	100	8.45	8.97	0.009	0.9728	11.17	0.011	0.757	0.517	0.9749

as well as a linearised form of pseudo-second-order kinetic equations was used to validate the data obtained in the kinetic studies. The results obtained after regression analysis of the data collected for the pseudo-first-order and pseudo-second-order kinetics are shown in Fig. 8(A) and (B), respectively. Applicability of any of the rate equation is decided based on the value of regression coefficient  $R^2$ . The  $R^2$  value of the pseudo-first-order equation, shown in Table 1, having higher value suggests that this could describe the adsorption of DR23 better than the pseudo-second-order equation with lower  $R^2$  values. This suggests that the adsorption process is dependent upon the concentration of the solute. The theoretical values of  $q_e$  that was calculated from the equation obtained for pseudo-first-order model shows a reasonably good agreement with experimental values of  $q_e$ . On the other hand, difference between calculated and experimental values of  $q_e$  for pseudo-second-order model was quite large.

The above two models cannot explain the mechanism of the adsorption process. Therefore, intra-particle diffusion model was employed to understand the mechanism of the adsorption. The higher values of correlation coefficient  $R^2$  listed in Table 1 suggest intra-particle diffusion is responsible for the adsorption of the dye molecules. However, the fact that the plot doesn't pass through the origin as shown in Fig. 8(C) implies that it is not the only controlling factor for adsorption of DR23 dye.

### 3.4. Effect of rotor speed on dye removal in RPB

Effect of rotor speed on the adsorption of the dye could be one of the most important factors as the centrifugal force which enhances the mass transfer rate in a RPB, varies with the speed at which the rotor spins. Three different values of rotor speed, namely, 628, 855 and 1,140 rpm at a constant feed rate of 20 Lh<sup>-1</sup> and 5 g of activated carbon loading were used in this work. The result shows almost similar per cent removal of dye except at 855 rpm after 2 h. Per cent

removal slightly decreased at rotor speed 855 rpm and it has the lowest adsorption capacity, 6.9 mg/g as evident from Fig. 9(A). Although per cent removal at 628 and 1,140 rpm are almost similar, they have different adsorption capacities. The highest adsorption capacity was observed at 628 rpm rotor speed and was calculated as 8.35 mg g<sup>-1</sup> of activated carbon loading. The reason for the decrease in adsorption at 855 rpm may be attributed to the fact that the solid mass of activated carbon shifts towards the outer wall of the rotor with increasing rotor speed thereby decreasing the path length of the liquid flow within activated carbon. The liquid profile inside the rotor also takes an "egg shell" like shape due to the centrifugal force [33]. This also contributes to the decrease in path length. With increasing rotational speed, the depth of the "egg shell" increases and path length decreases further. In this case, the increase in mass transfer coefficient due to increasing centrifugal force [29] cannot compensate for the effect of decrease in liquid flow path length. However, when the rotor speed is increased further, the adsorption again increases. In this case, the increase in the mass transfer coefficient predominates over the decrease in path length due to displacement of the activated carbon and the water profile towards outer wall of the rotor [28].

### 3.5. Effect of feed rate on dye removal in RPB

Feed rate is one of the parameters that can affect the adsorption characteristics of DR23 in a RPB. Adsorption behaviour was observed for four different feed rates namely; 10, 20, 30 and 40 Lh<sup>-1</sup> at the same rotor speed, 855 rpm and 5 g of activated carbon loading. The liquid was recirculated from a reservoir containing 1 L of the dye solution. It can be seen in the Fig. 9(B), 82 and 80% of dye removal were obtained at feed rates 40 and 30 Lh<sup>-1</sup>, respectively, and 67 and 63% of dye removed at 20 and 10 Lh<sup>-1</sup>, respectively. Adsorption capacity did not vary for feed rates, 30 and 40 Lh<sup>-1</sup>, which was 9 mg/g. Adsorption data at feed rates 10 and 20 Lh<sup>-1</sup> were very close in the first hour but feed

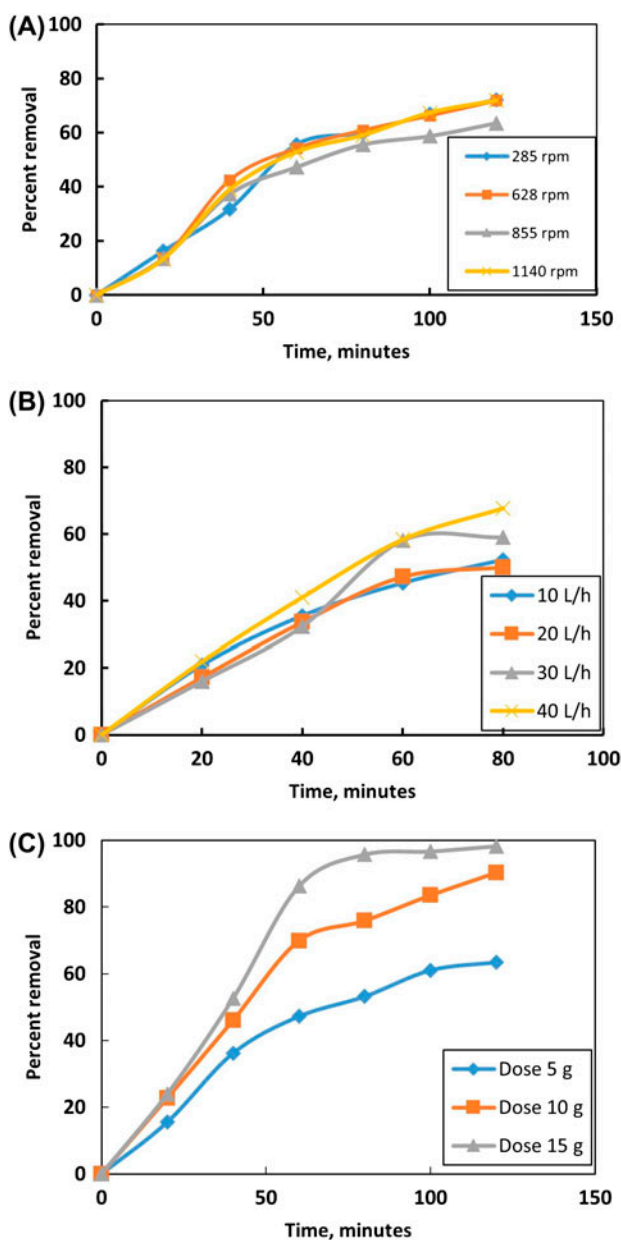


Fig. 9. (A) Effect of rotor speed, (B) effect of feed rate and (C) effect of activated carbon loading on adsorption of DR23.

rate of  $10 \text{ L h}^{-1}$  showed higher adsorption in the following hour. However, despite this anomaly, higher feed rate generally increases the probability of contact between the activated carbon and liquid, which in turn increases the adsorption of the dye.

### 3.6. Effect of activated carbon loading on dye removal in RPB

In order to investigate the effect of activated carbon dose, experiments were carried out in three different

loadings, 5, 10 and 15 g which correspond to 255, 510, 765  $\text{kg m}^{-3}$ , respectively, at the same rotor speed and feed rate. It can be observed from Fig. 9(C) that the percent removal increased with higher activated carbon loading because of the availability of more adsorption sites. With increasing amount of activated carbon loading, the packing is more compact and there is less distortion of the pack due to high speed rotation. This ensures that the path length travelled by the liquid is higher than that for low compaction when less quantity of activated carbon is used.

## 4. Conclusion

Adsorption of DR23 on activated carbon in a high gravimetric RPB contactor was tested successfully. The centrifugal force generated in the RPB enhanced the removal of the dye due to reduced mass transfer resistance. The adsorption was fast and within 5 h, almost 93% dye was removed compared to 54% in the traditional shake flask experiment during the same period of time. Rotating speed of the rotor and liquid feed rate had significant effect on the removal of the dye. The process could be scaled up to suit industrial applications as this piece of equipment is already in use as a gas-liquid contactor in industry. Thus, RPB also provides a suitable alternative to conventional treatment methods for tertiary treatment of wastewater.

## Acknowledgements

The authors are grateful to the University of Malaya (project no. UM.C/HIR/MOHE/ENG/13 and IPPP project no. PG040-2012B) for providing the fund for the research work.

## References

- [1] H.R. Guendy, Enhancing of textile wastewater treatment using different catalysts for advanced oxidation process, *Aust. J. Basic Appl. Sci.* 3 (2009) 4046–4052.
- [2] M. Kazemi, J.S.S. Mohammadzadeh, A.B. Khoshfetrat, M.A. Kaynejad, Decolorization of RR-120 dye using ozone and ozone/UV in a semi-batch reactor, *Can. J. Chem. Eng.* 82 (2004) 1284–1288.
- [3] M. Neamtu, A. Yediler, I. Siminiceanu, M. Macoveanu, A. Kettrup, Decolorization of disperse red 354 azo dye in water by several oxidation processes—A comparative study, *Dyes Pigm.* 60 (2004) 61–68.
- [4] H.-Y. Shu, C.-R. Huang, Degradation of commercial azo dyes in water using ozonation and UV enhanced ozonation process, *Chemosphere* 31 (1995) 3813–3825.
- [5] L. Szyrkowicz, C. Juzzolino, S.N. Kaul, A Comparative study on oxidation of disperse dyes by electrochemical process, ozone, hypochlorite and Fenton reagent, *Water Res.* 35 (2001) 2129–2136.

- [6] J. Wu, T. Wang, Ozonation of aqueous azo dye in a semi-batch reactor, *Water Res.* 35 (2001) 1093–1099.
- [7] T. Robinson, G. McMullan, R. Marchant, P. Nigam, Remediation of dyes in textile effluent: A critical review on current treatment technologies with a proposed alternative, *Bioresour. Technol.* 77 (2001) 247–255.
- [8] U.K. Khare, P. Bose, P.S. Vankar, Impact of ozonation on subsequent treatment of azo dye solutions, *J. Chem. Technol. Biotechnol.* 82 (2007) 1012–1022.
- [9] J. Shore, Advances in direct dyes, *Indian J. Fibre Text.* 21 (1996) 1–29.
- [10] S. Song, L. Xu, Z. He, H. Ying, J. Chen, X. Xiao, B. Yan, Photocatalytic degradation of C.I. Direct Red 23 in aqueous solutions under UV irradiation using SrTiO<sub>3</sub>/CeO<sub>2</sub> composite as the catalyst, *J. Hazard. Mater.* 152 (2008) 1301–1308.
- [11] S. Song, H. Ying, Z. He, J. Chen, Mechanism of decolorization and degradation of CI Direct Red 23 by ozonation combined with sonolysis, *Chemosphere* 66 (2007) 1782–1788.
- [12] N. Daneshvar, D. Salari, A. Niaei, M. Rasoulifard, A. Khataee, Immobilization of TiO<sub>2</sub> nanopowder on glass beads for the photocatalytic decolorization of an azo dye CI Direct Red 23, *J. Environ. Sci. Health A Tox. Hazard. Subst. Environ. Eng.* 40 (2005) 1605–1617.
- [13] N. Sobana, K. Selvam, M. Swaminathan, Optimization of photocatalytic degradation conditions of Direct Red 23 using nano-Ag doped TiO<sub>2</sub>, *Sep. Purif. Technol.* 62 (2008) 648–653.
- [14] M. Sohrabi, M. Ghavami, Photocatalytic degradation of Direct Red 23 dye using UV/TiO<sub>2</sub>: Effect of operational parameters, *J. Hazard. Mater.* 153 (2008) 1235–1239.
- [15] A.C. Lucilha, C.E. Bonancêa, W.J. Barreto, K. Takashima, Adsorption of the diazo dye Direct Red 23 onto a zinc oxide surface: A spectroscopic study, *Spectrochim. Acta A* 75 (2010) 389–393.
- [16] W. Konicki, I. Pelech, E. Mijowska, I. Jasińska, Adsorption of anionic dye Direct Red 23 onto magnetic multi-walled carbon nanotubes-Fe<sub>3</sub>C nanocomposite: Kinetics, equilibrium and thermodynamics, *Chem. Eng. J.* 210 (2012) 87–95.
- [17] F. Doulati Ardejani, K. Badii, N. Yousefi Limaee, M. Arami, S. Shafaei, A. Mirhabibi, Numerical modelling and laboratory studies on the removal of Direct Red 23 and Direct Red 80 dyes from textile effluents using orange peel, a low-cost adsorbent, *Dyes Pigm.* 73 (2007) 178–185.
- [18] C.-C. Lin, B.-C. Chen, Carbon dioxide absorption in a cross-flow rotating packed bed, *Chem. Eng. Res. Des.* 89 (2011) 1722–1729.
- [19] C. Ramshaw, R.H. Mallinson, Mass Transfer Process, U.S. Patent No. US4283255 A, USA, 1981.
- [20] D.P. Rao, A. Bhowal, P.S. Goswami, Process intensification in rotating packed beds (HIGEE): An appraisal, *Ind. Eng. Chem. Res.* 43 (2004) 1150–1162.
- [21] A. Mondal, A. Pramanik, A. Bhowal, S. Datta, Distillation studies in rotating packed bed with split packing, *Chem. Eng. Res. Des.* 90 (2012) 453–457.
- [22] C.-C. Lin, T.-J. Ho, W.-T. Liu, Distillation in a rotating packed bed, *J. Chem. Eng. Jpn.* 35 (2002) 1298–1304.
- [23] H. Zhao, L. Shao, J.-F. Chen, High-gravity process intensification technology and application, *Chem. Eng. J.* 156 (2010) 588–593.
- [24] L.-L. Zhang, J.-X. Wang, Y. Xiang, X.-F. Zeng, J.-F. Chen, Absorption of carbon dioxide with ionic liquid in a rotating packed bed contactor: Mass transfer study, *Ind. Eng. Chem. Res.* 50 (2011) 6957–6964.
- [25] C.-Y. Chiang, Y.-S. Chen, M.-S. Liang, F.-Y. Lin, C.Y.-D. Tai, H.-S. Liu, Absorption of ethanol into water and glycerol/water solution in a rotating packed bed, *J. Taiwan Inst. Chem. Eng.* 40 (2009) 418–423.
- [26] L.-J. Hsu, C.-C. Lin, Binary VOCs absorption in a rotating packed bed with blade packings, *J. Environ. Manage.* 98 (2012) 175–182.
- [27] C.-C. Lin, H.-S. Liu, Adsorption in a centrifugal field: Basic dye adsorption by activated carbon, *Ind. Eng. Chem. Res.* 39 (1999) 161–167.
- [28] A. Das, A. Bhowal, S. Datta, Continuous biosorption in rotating packed-bed contactor, *Ind. Eng. Chem. Res.* 47 (2008) 4230–4235.
- [29] M. Panda, A. Bhowal, S. Datta, Removal of hexavalent chromium by biosorption process in rotating packed bed, *Environ. Sci. Technol.* 45 (2011) 8460–8466.
- [30] A. Kundu, G. Redzwan, J.N. Sahu, S. Mukherjee, B.S. Gupta, M.A. Hashim, Hexavalent chromium adsorption by a novel activated carbon prepared by microwave activation, *Bioresources* 9 (2014) 1498–1518.
- [31] S. Kushwaha, S. Sodaye, P. Padmaja, Equilibrium, kinetics and thermodynamic studies for adsorption of Hg(II) on palm shell powder, *Proceedings of World Academy of Science, Engineering and Technology*, 2008, pp. 617–623.
- [32] S. BioScience, RPM vs. RCF, 2014. Available from: <<http://www.sorbio.com/index.php/rpm-vs-rcf>>.
- [33] V. Lubarda, The shape of a liquid surface in a uniformly rotating cylinder in the presence of surface tension, *Acta Mech.* 224 (2013) 1365–1382.